Chemistry SELECT

www.chemistryselect.org

A journal of ChemPubSoc Europe

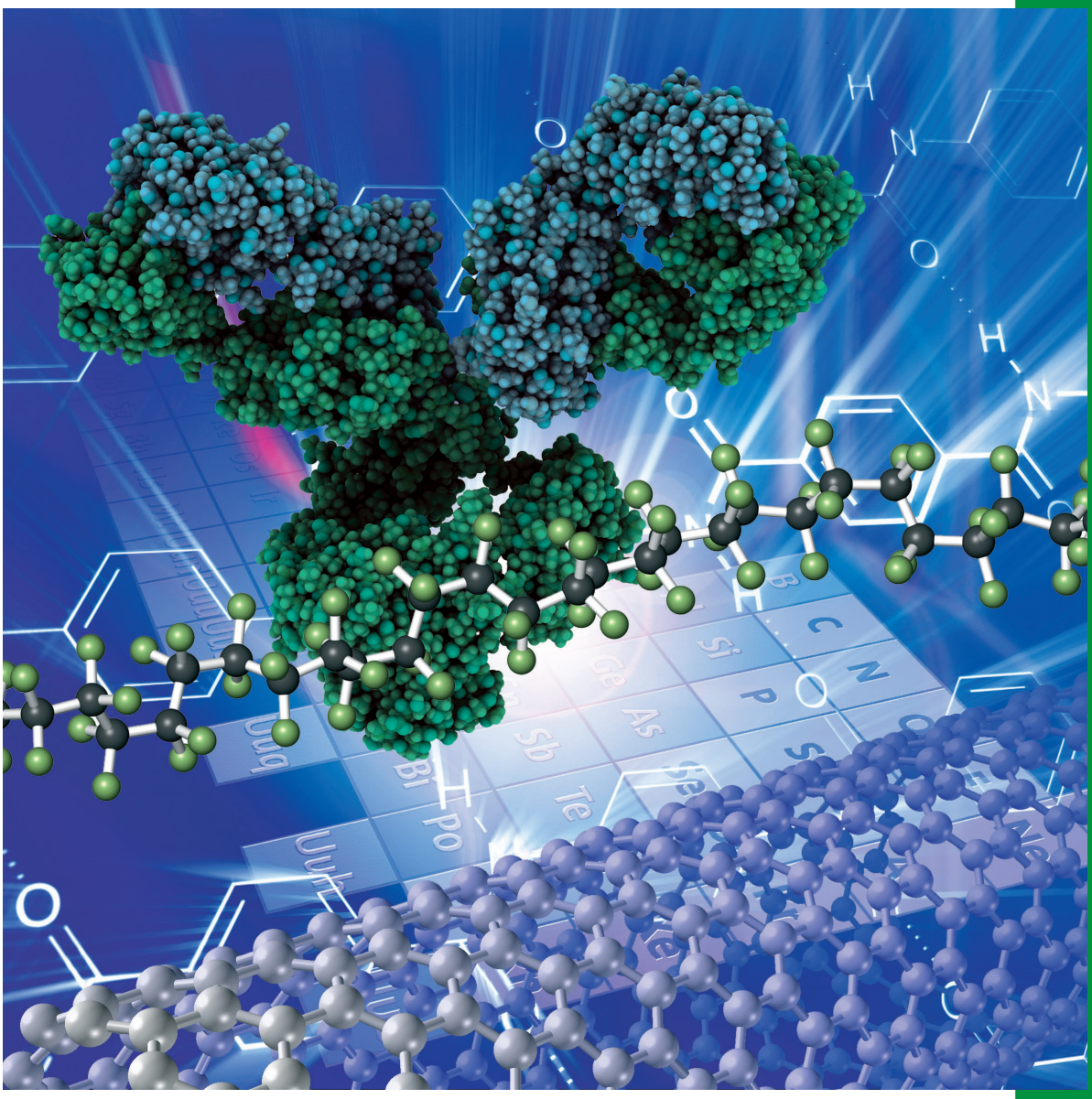

REPRINT

WILEY-VCH

ChemPubSoc Europe

DOI: 10.1002/slct.201900046

Chemistry SELECT Full Papers

Electro, Physical & Theoretical Chemistry

Synthesis, Water-Removing Method and Influences of Trace Water for $LiBF_4$

Dongni Zhao,[a, b] Dan Lei,[a, b] Peng Wang,[a, b] Shiyou Li,[a, b, c] Haiming Zhang,[c] and Xiaoling Cui*[a, b]

Recent works show the promise for lithium tetrafluoroborate ($LiBF_4$) as an electrolyte salt for lithium-ion batteries. In this paper, $LiBF_4$ is synthesized by a novel reaction between the as-prepared anhydrous Li_2SO_3 and $(C_2H_5)_2O{\cdot}BF_3$ in an aprotic solvent. The moisture sensitivity and water-removing method of $LiBF_4$ materials which has been dried under vacuum for 2 h at different temperature, is studied by Fourier transform infrared spectroscopy measurements. Results show that almost all of the adsorbed water would be removed at above 65 °C. With the increase of drying temperature, crystal water will decrease slowly, and almost disappear completely at 170 °C. However, due to the thermal decomposition of $LiBF_4$, LiF and BF_2OH impurities are formed as the temperature reaches 165 °C. So, we determine that the proper drying temperature is 155 °C, though the trace water cannot be removed thoroughly. Besides, influences of trace water on the electrochemical performance of Li/MCMB half-cell with $LiBF_4$ as electrolyte salt has been investigated. Results show that discharge plateaus at about 1.5 V vs. Li/Li^+ will be lengthened with the increase of water content. Subsequently, the so-called solid-electrolyte interphase (SEI) film will become thicker and more resistant, which leads to poor Li^+ ion migration and bad cycling performance.

1. Introduction

With the energy crisis approaches, new energy storage materials continue to rise. Lithium ion battery (LIBs) as one of the most appropriate material has drawn the intensive attention with the advantage of superior energy/power density, long cycle life, less memory effect, and low self-discharging rate.[1–3] Lithium salt-based electrolyte is an indispensable component in LIBs. It serves as a carrier ion-conductive and electron-insulating medium facilitating Li^+ ions transport between cathode and anode electrodes, simultaneously holding important implications for LIBs' performances, such as low temperature circulation and security properties.[4,5]

Non-aqueous electrolyte as "blood" in lithium-ion batteries plays as a porter of lithium ions between the positive and negative electrodes. Therefore, it needs to have many feature, including high conductivity over a wide range of temperature, low impedance of passivation layers, good ability to passivate the aluminum current collector as well as wide electrochemical stability.[6–8] Most commonly, anhydrous electrolyte systems containing $LiPF_6$ salt in ethylene carbonate (EC) as cyclic carbonate and dimethyl carbonate (DMC) as linear carbonate are used for commercial LIBs.[9,10] However, $LiPF_6$ is thermally unstable and easy to suffer hydrolysis reaction with trace water. Considering the defect of $LiPF_6$, $LiBF_4$ with the structure ascendancy, which has stronger inter and intra molecular forces, can act as substitution of $LiPF_6$. The B–F bond in $LiBF_4$ is less labile than the P–F bond in $LiPF_6$, resulting in improved hydrolytic and thermal stability of electrolyte solutions.[11,13] Besides, $LiBF_4$ has been confirmed that several other key advantages over $LiPF_6$, such as its improved performance at sub-zero temperatures, improved passivation of the Al current collector, and improved performance at the positive electrode.[18] Xu have stated that $LiBF_4$-based electrolyte show outstanding performance, not only at elevated temperature up to 50 °C, but surprisingly, also at low temperature and high discharge rate as well, which is usually ascribed to its relatively higher conductivity and smaller charge-transfer resistance than $LiPF_6$ under such harsh circumstance.[19] Hence, $LiBF_4$ electrolytes have already attracted renewed attention for LIBs.[20,21]

A green procedure method to prepare $LiBF_4$ without any use of organic solvent was developed, as shown in Equation (1) and (2).[22]

$$4HF + H_3BO_3 \rightarrow HBF_4 + 3H_2O, \quad (1)$$

$$2HBF_4 + Li_2CO_3 \rightarrow 2LiBF_4 + H_2O + CO_2. \quad (2)$$

However, it is apt to bring in the impurity of water which will dramatically damage the performance of LIBs. Not only

[a] Dr. D. Zhao, D. Lei, Dr. P. Wang, Prof. S. Li, Prof. X. Cui
College of Petrochemical Technology, Lanzhou University of Technology, Lanzhou 730050, China
Tel.: +86-931-2973305
Fax: +86-931-2973648
E-mail: xlcuilw@163.com
[b] Dr. D. Zhao, D. Lei, Dr. P. Wang, Prof. S. Li, Prof. X. Cui
Gansu Engineering Laboratory of Electrolyte Material for Lithium-ion Battery, Lanzhou 730050, China
[c] Prof. S. Li, H. Zhang
Qinghai Research Center of Low-temperature Lithium-ion Battery Technology Engineering, Qinghai Green Grass New Energy Technology Co. Ltd., Xining, 810000, P.R. China

Supporting information for this article is available on the WWW under https://doi.org/10.1002/slct.201900046

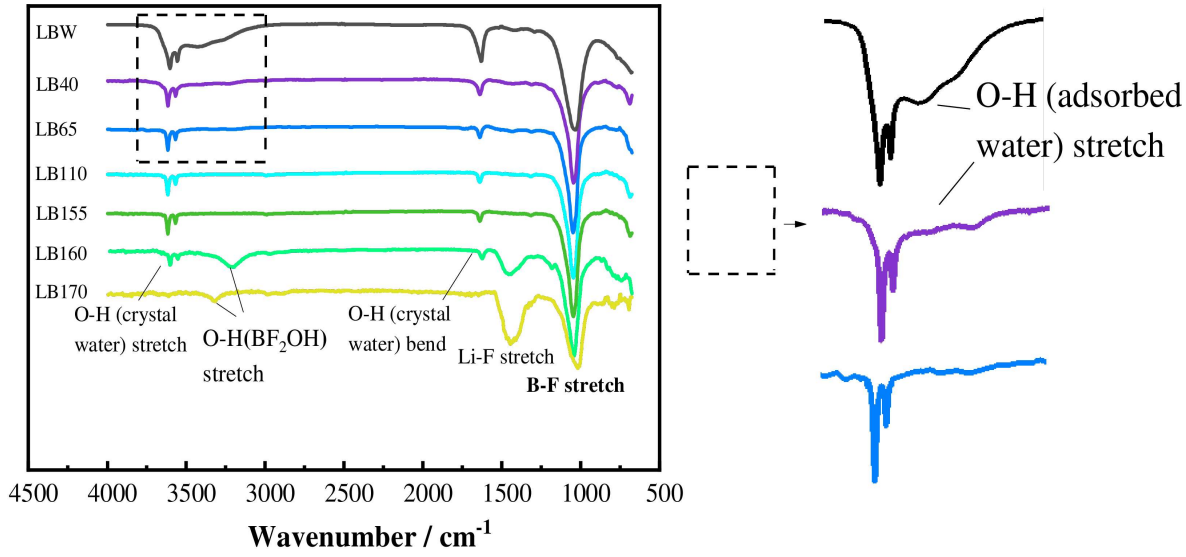

Figure 1. FT-IR spectra of $LiBF_4$ dried with different temperatures

does it react with anode material, but unfriendly hydrolysis products generate when touched with lithium salt.[23] For example, products of B_2O_3, LiF and HF are produced by the decomposition of $LiBF_4$, which deposited on the SEI film surface of the anode electrode. The insoluble products will deposit on the surface of electrode, making the so-called solid-electrolyte interphase (SEI) film become thicker and more resistant. Besides, the acid will impact seriously on cathode electrode with corrosion effect, reducing cycling performance and leading to security problem.[24] Therefore, the water content of lithium salts should be reduced as much as possible to minimize the detrimental reactions in batteries.[25]

In this paper, $LiBF_4$ is prepared by a novel green procedure method. Besides, the relation between drying temperature and water content will be studied to find optimum water-removing method. In addition, to further clarify the mechanism of water action, influences of trace water on the electrochemical performance of MCMB/Li half cell with $LiBF_4$ as electrolyte salt has been investigated.

2. Experimental

The corresponding experiment details are given in Supporting Information.

3. Results and Discussion

3.1 FT-IR spectra of $LiBF_4$ and water contents measurement

FT-IR is used to track the evolution of characteristic vibrational modes after different drying temperature. Five important regions are shown in Figure 1, which are attributed to the B–F stretching mode (1033 cm^{-1}),[26] O–H bending mode of crystal water (1635 cm^{-1}), O–H stretching mode of adsorbed water (about 3300 cm^{-1}) and O–H stretching mode of crystal water (3617 cm^{-1}), respectively. It should be noted that for the $LiBF_4$ solid which has been dried at 40 °C for 2 h (LB40), a blurry wide O–H stretching signal at about 3300 cm^{-1} appears, indicating the existence of adsorbed water. And this deduction has been verified by the fact that this signal becomes more obvious with the increase of adsorbed water, as shown in the spectrum for LBW. Besides, we can deduce that almost all of the adsorbed water would be removed for samples dried at above 65 °C, based on the phenomenon that the O–H stretching signal at about 3300 cm^{-1} has been disappeared.

With the increase of drying temperature, characteristic peaks for crystal water will decrease slowly, and almost disappear completely at 170 °C. However, it should be noted that new signals at ~1427 cm^{-1} and 3200~3300 cm^{-1} appear when the temperature is higher than 155 °C, attributed to Li–F stretching mode and O–H stretching vibration for BF_2OH,[27] respectively. That is, due to the thermal decomposition of $LiBF_4$, LiF and BF_2OH impurities are formed as the temperature reaches 160 °C, according to the equations listed as follows,

$$LiBF_4 \rightarrow BF_3 + LiF, \quad (4)$$

$$BF_3 + H_2O \rightarrow BF_2OH + HF. \quad (5)$$

So, we determine that the proper drying temperature is 155 °C, though the trace water cannot be removed thoroughly. That is, it is hard to prepare pure water-free $LiBF_4$ by common vacuum drying method. To make quantitative analysis, the water content of LBW, LB110 and LB155 samples are measured by Karl–Fischer titration, and the results are shown in Table 1. It indicates that it is hard to make water content become less than 55.6 ppm for dried $LiBF_4$ product.

Table 1. Water contents of three $LiBF_4$ samples			
Sample	LBW	LB110	LB155
Water content /ppm	9743.8	3453.3	55.6

3.2 Quantum chemistry (QC) calculation

FT-IR spectra for $LiBF_4$ materials with different number of crystallized water were obtained by QC calculation, as shown in Figure 2. Obviously, in the so called "fingerprint region" range of 1350 ~ 400 cm^{-1}, many stretching vibrations belonging to various single bonds and the bending vibrations of majority groups (e.g., B–F, O–H bonds, etc.) have been obtained by QC calculation.

Besides, as we all know, the types of vibrations in this region are complex, overlapping and poor characteristics, due to the fact that they are highly sensitive to changes in molecular structure. With minor changes in molecular structure, significant changes will be taken in this part of the spectrum. In the range of 880 ~ 1314 cm^{-1}, three characteristic peaks have arisen from three modes of vibration for B–F bonds, corresponding to B atom vibration in the direction of x-axis, z-axis, and 45° angle between x- and y-axes, as has been diagramed in Figure 2. We can infer that the most probable existence state for crystal water with $LiBF_4$ is $LiBF_4{\cdot}H_2O$, by comparing the QC calculation results with LB155 for peak shape and peak shift. That is, dried product for LB155 contains a large amount of $LiBF_4$ and very tiny amount of $LiBF_4{\cdot}H_2O$.

3.3 Initial discharge curves and cycling performance of Li/MCMB cells

It is well known that trace water will result in loss of irreversible capacity, corrosion for cathode materials, harm for cycle life, and damage for safety. To further clarify the mechanism of water action, the initial charge and discharge curves and cycling performance of Li/MCMB cells with $LiBF_4$-based electrolyte were studied.

The initial discharge curves of Li/MCMB cells with different electrolyte systems cycled at the current density of 0.026 mA cm^{-2} are presented in Figure 3. Two obvious discharge plateaus at about 1.8 V and 1.5 V are observed in the discharge curve of the electrode in three electrolyte systems. The 1.8 V plateau is due to a reductive decomposition of $LiBF_4$. The discharge specific capacity of 1.5 V plateau from LBW, LB110 and LB155 accounted for 1.38%, 0.56% and 0.34% of the total discharge specific capacity, the longer plateau of LBW is due to the increase in moisture eventually resulting in greater interface resistance.

Figure 4 shows the cycling performances of Li/MCMB cells for different electrolytes. It can be proved that the discharge capacity of three electrolyte systems at first cycle is much larger than that at second cycle, which is attributed to the forming of solid electrolyte interphase (SEI) on the Li surface at first cycle. Furthermore, LBW electrolyte causes severe capacity decay upon cycling, whereas LB155 electrolyte enables the stable charge discharge reaction over 50 cycles. The discharge capacity of the cell with LB155 and LB110 electrolyte is respectively 219.8 and 172.2 mAh g^{-1} after 50 cycles, but only 26.8 mAh g^{-1} discharge capacities is obtained from the Li/MCMB cell with LBW electrolyte after 50 cycles. This poorer of cycle performance of LBW electrolyte is attributed to the longer 1.5 V discharge plateau caused by the increase of moisture. The solid electrolyte interphase (SEI) film mostly consists of Li_2CO_3 and LiF, when moisture content is more than the required content of the formation of SEI, H_2O can react with Li_2CO_3 to produce gas and make the topical surface of SEI film not dense and even. In addition, H_2O can react with $LiBF_4$ to generate B_2O_3 and LiF precipitation deposited on SEI film surface of the anode electrode, which makes SEI film become thicker and shows an increased battery internal resistance, higher interface

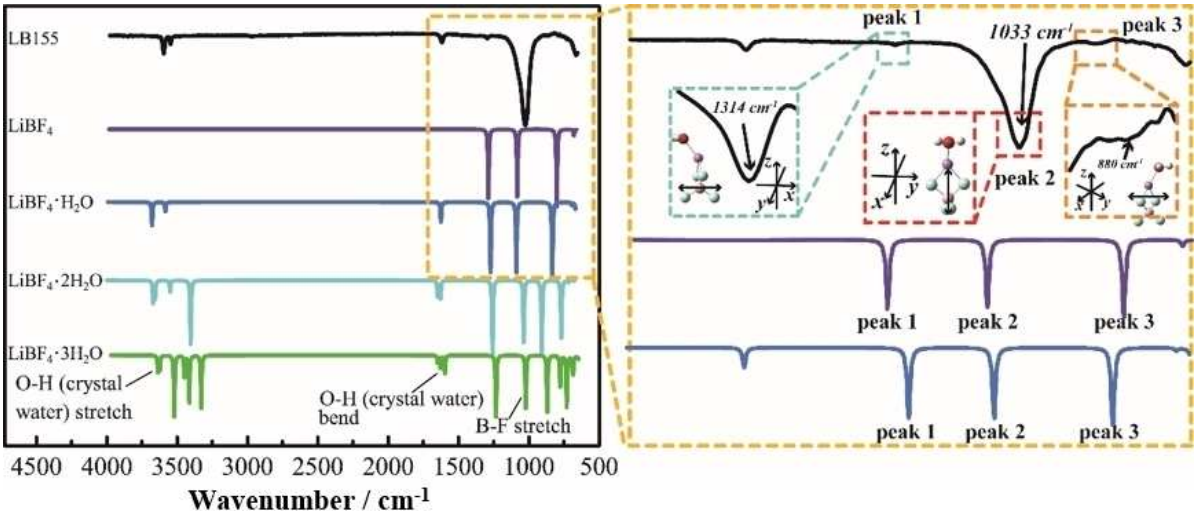

Figure 2. FT-IR spectra for $LiBF_4$ with different number of crystallized water obtained by QC calculation.

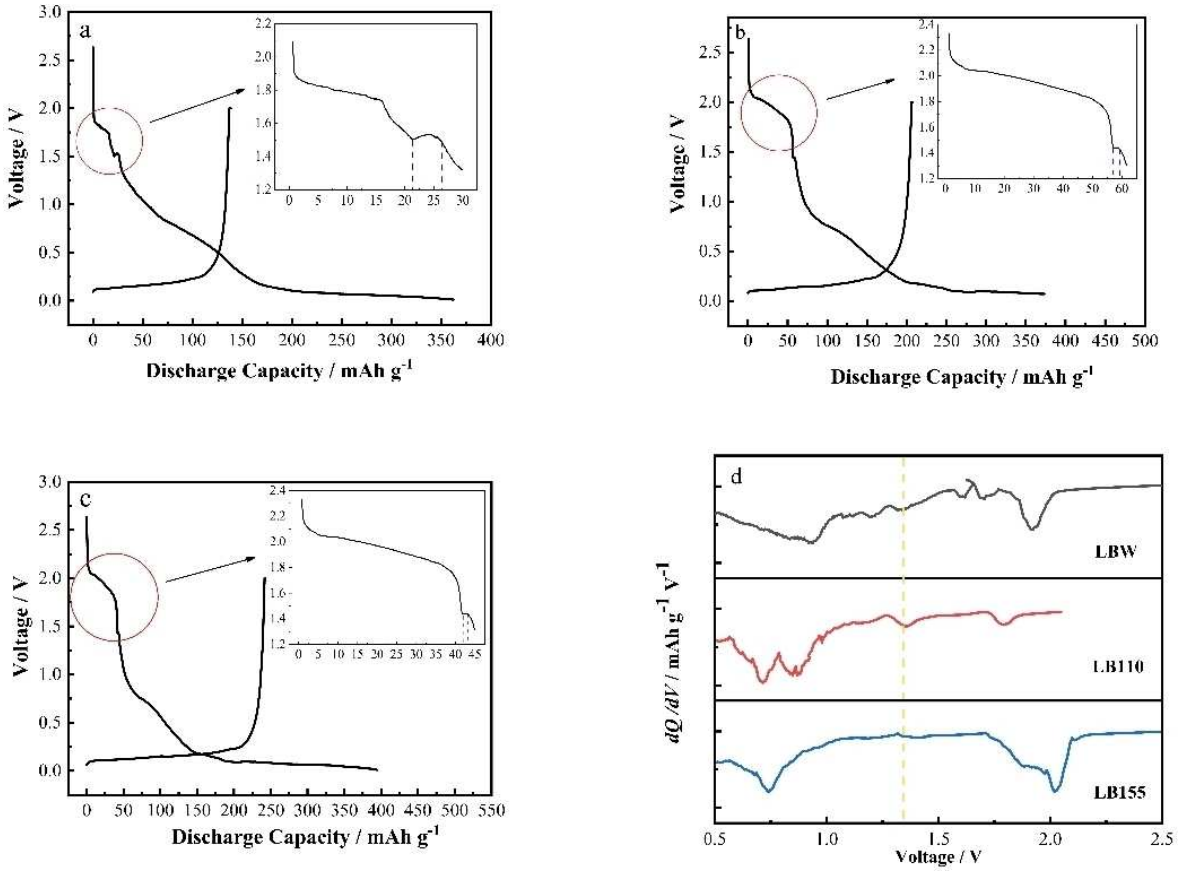

Figure 3. Initial discharge curves of Li/MCMB cells with (a) LBW electrolyte, (b) LB110 electrolyte and (c) LB155 electrolyte; (d) Differential capacity curve of different electrolytes

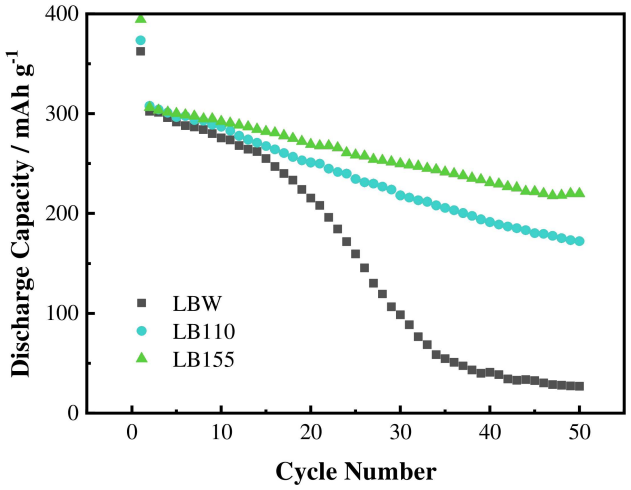

Figure 4. Cycling performances of Li/MCMB cells at 0.01-2.0 V for different electrolytes.

resistance and worse Li^+ migration, this greatly deteriorates the cycling performance for the cells of LBW electrolyte.[28]

3.4 Impedance analysis

To probe the obstruction of SEI film, impedance of Li/MCMB cells in three electrolytes are tested at 25 °C, which is drawn in Figure 5. There are three main parts in the impedance spectrum. Ohmic resistance (R_s), which is representative of the contact resistance between electrolyte and cell, comes from the intercept in the high frequency of impedance spectra. The key section to evaluate the properties of electrolyte depends on R_f in the impedance, which represent the impedance value of the lithium-ion migration through the multilayer surface film. R_f mainly obtains information from the semicircle in the middle region of the impedance spectrum. The final section is the slop line at low frequency pointed to the charge transfer resistance (R_{ct}) and Warburg diffusion (W).[29] For the reason that considering the effect of lithium foil on the impedance, the R_f and R_{ct} can be taken as a relative measure of the resistances to make a comparison of the surface resistance and charge transfer resistance of the working electrode.

Resultant R_s, R_f and R_{ct} are summarized in Table 2. The changes in both R_f and R_{ct} are in the order of LBW > LB110 > LB155. This is exactly opposite to the order of performance. Optimal cycling performance of LB155 is thus ascribed to the effective surface passivation by a thinner and stable SEI layer

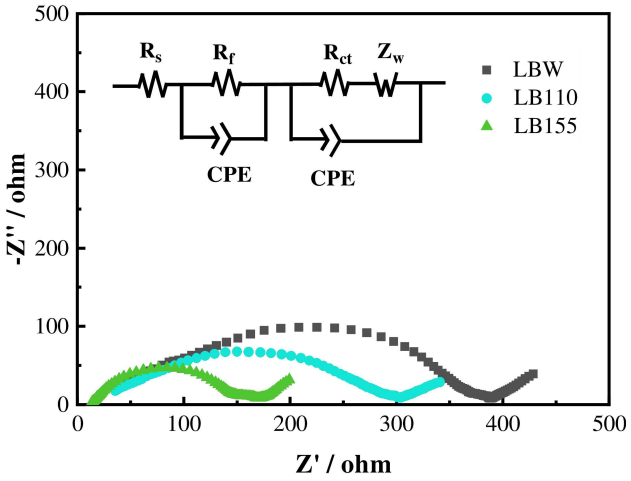

Figure 5. Impedance spectra of Li/MCMB cells with different electrolytes at initial fully lithiated state and corresponding equivalent circuit.

Table 2. Simulated result for the elements of equivalent circuit

Sample	R_s	R_f	R_{ct}
LBW	8.05	227.9	149.98
LB110	10.57	166.6	120.5
LB155	9.62	97.05	75.5

that is composed of less resistive surface species. After water absorption, a distinct increase of the MCMB electrode surface impedance is observed in cell of LBW electrolyte. This is most probably due to B_2O_3 and LiF precipitation deposited on the SEI film surface of the anode electrode. The high impedances of surface layer and charge transfer of the electrode with LBW electrolyte increase ohmic polarization and activation polarization during over and over again lithiation/delithiation,[30] confirming the above mentioned inferior electrochemical performance with LBW electrolyte.

3.5 SEM analyses

To further investigate the effects of absorbed water on the MCMB electrode, SEM analysis were performed after first fully discharge of the Li/MCMB cells, as shown in Figure 6. It is observed that the foreign materials are deposited on the three electrode surfaces, due to the formation of (SEI film) deposited by electrolyte decomposition. Compared with the compact surface of MCMB electrode of LB155 electrolyte, there are some cracks among the particles of the electrode of LBW electrolyte, which can increase surface area and result in the interface reaction. The crack and untight surface of LBW electrolyte is due to H_2O can react with SEI film component (Li_2CO_3) to produce gas and make the topical surface of SEI film not become dense and even. In comparison, the MCMB surface cycled in LB155 sample shows a compact surface. The particles of the MCMB electrode are smooth and the surface is flat, which is ascribed to the film of MCMB electrode with LB155 electrolyte is stably formed.

3.6 XPS analysis

In order to understand the specific composition of the SEI film derived from the MCMB surface layer between electrode with LB155 electrolyte and with LBW electrolyte, XPS patterns are obtained after first cycles as displayed in Figure 7. Three main peaks in the C 1s spectra are detected: C–C bond belonging to carbon black (284.5 eV), C–H bond due to lithium alkyl carbonates (R–CH_2OCO_2–Li) (285.8 eV), C=O bond in lithium alkyl carbonates (R–CH_2OCO_2–Li) and polycarbonates (289.5 eV). In the F 1s spectra, three peaks at binding energies (BEs) of 688.7, 686.4 and 685.3 eV, respectively, are detected. These peaks are assigned to polyvinylidene difluoride (PVDF),[31] decomposition products of BF_4^-[32] and LiF,[33] and the content of the LiF of LBW sample is more than LB155. LiF, which has poor conductive property, can influence the electrochemical performance of cell. As for O 1s, the peak around 531.4 eV can be assigned to the Li_2CO_3[34] and its peak intensity in LB155 sample is weaker than that in LBW sample. The results demonstrate that Li_2CO_3 of the cell of LBW electrolyte are consumed by water to produce gas, thus destroying the surface of SEI film.[35–37] The B 1s spectrum shows two peaks at 192 and 190.8 eV attributed to B_2O_3 and B–F, respectively, B–F bond are attributed to the decomposition products of BF_4^-. The intensity of the B_2O_3 peak with LBW sample is the stronger than LB155 sample, the result corroborates the observation of EIS spectra.

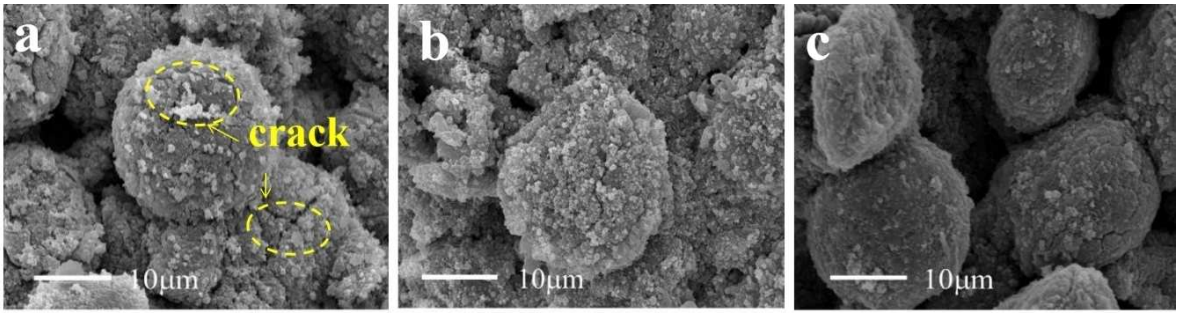

Figure 6. SEM images of surface morphologies of MCMB electrodes at firstly fully lithiated state. a) LBW electrolyte, (b) LB110 electrolyte and (c) LB155 electrolyte.

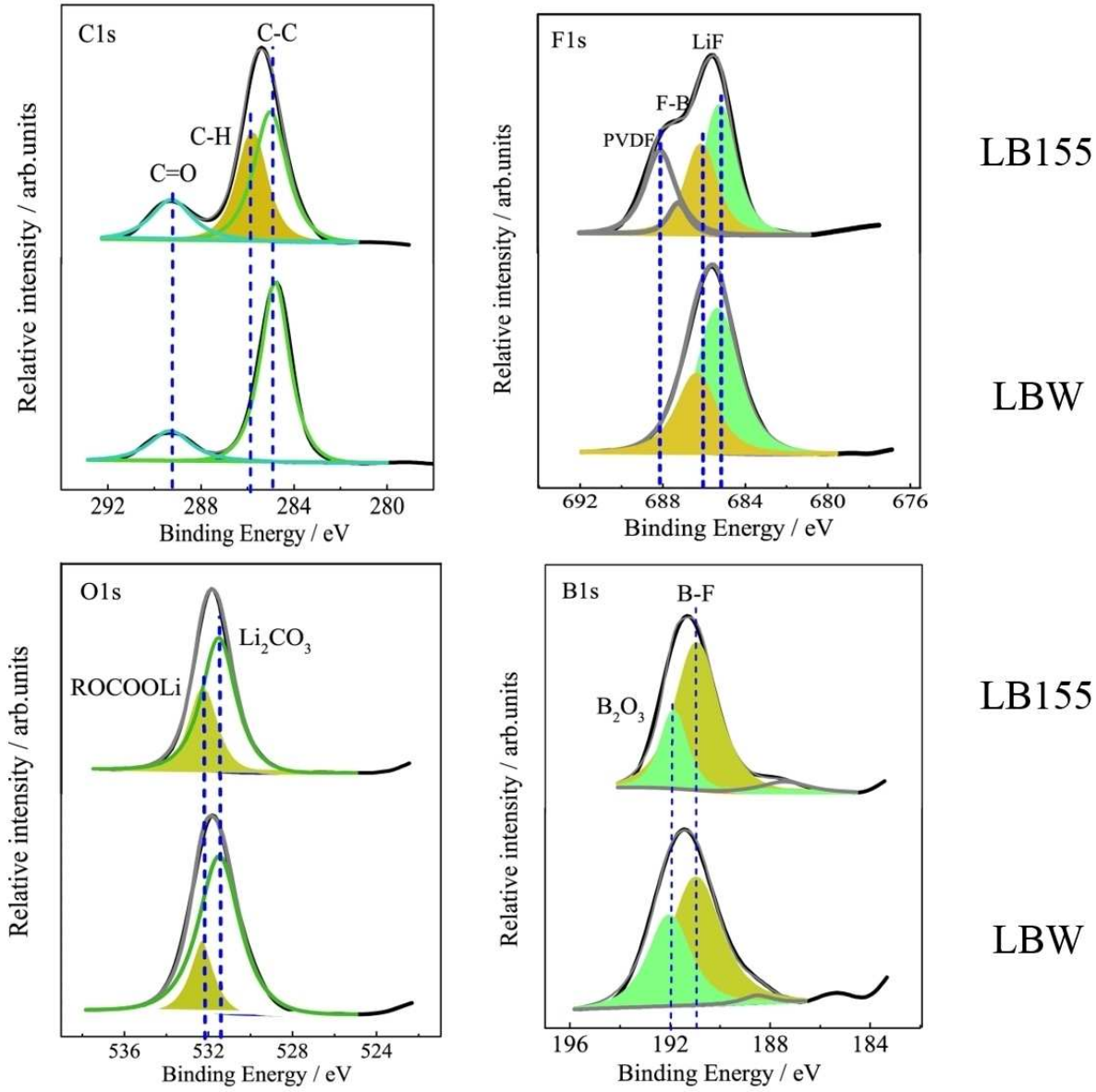

Figure 7. XPS spectra of MCMB electrodes at firstly fully lithiated state.

After absorbing water with $LiBF_4$ sample, H_2O can react with $LiBF_4$ to generate B_2O_3 precipitation deposited on SEI film surface of the anode electrode, increasing interface resistance. Accordingly, lithium-ion batteries exhibit inferior cycling capabilities with LBW electrolyte.

4. Conclusions

$LiBF_4$ was investigated as a salt for the electrolyte in LIBs several years ago. First, our work gives a novel synthesis method for $LiBF_4$ salt. Second, we have found that it is hard to prepare pure water-free $LiBF_4$ by common vacuum drying method, and we determine the condition of 155 °C for 2 h under vacuum as the proper water-removing method. At last, we have found that trace water has great damage for cell performance, due to its negative effect on SEI film.

Supporting Information Summary

The complete Experimental Section is available in the Supporting Information.

Acknowledgements

This work was supported by the Natural Science Foundation of China (No. 21766017), Science and Technology Project for Gansu Province (No. 18JR3RA160) and Lanzhou university of technology hongliu first-class discipline construction program.

Conflict of Interest

The authors declare no conflict of interest.

Keywords: $LiBF_4$ · Water-removing method · SEI film · Lithium-ion batteries · Electrolyte

[1] S. Kim, M. Kim, I. Choi, J. J. Kim, *J. Power Sources.* **2016**, *336*, 316-324.
[2] W. Luo, B. Zheng, *Appl. Surf. Sci.* **2017**, *404*, 310-317.
[3] Y. Luo, T. Lu, Y. Zhang, L. Yan, J. Xie, S. S. Mao, *J.Power Sources.* **2016**, *323*, 134-141.
[4] Y. Yamada, A. Yamada, *J. Electrochem. Soc.* **2015**, *162*, A2406-A2423.
[5] M. T. Ong, O. Verners, E. W. Draeger, A. C. van Duin, V. Lordi, J. E. Pask, *J. Phys. Chem. B.* **2015**, *119*, 1535-1545.
[6] R. Chen, Y. Chen, L. Zhu, Q. Zhu, F. Wu, L. Li, *J. Mater. Chem. A.* **2015**, *3*, 6366-6372.
[7] M. Kerner, D.-H. Lim, S. Jeschke, T. Rydholm, J.-H. Ahn, J. Scheers, *J. Power Sources.* **2016**, *332*, 204-212.
[8] K. Xu, *Chem Rev.* **2004**, *104*, 4303-4418.
[9] R. A. Guidotti, B. J. Johnson, *Office of Scientific & Technical Information Technical Reports*, **2015**.
[10] J. Yang, S. C. Wang, X. Y. Zhou, J. Xie, *Int. J. Electrochem. Sc.* **2012**, *7,* 6118–6126.
[11] T. R. Jow, M. S. Ding, K. Xu, S. S. Zhang, J. L. Allen, K. Amine, G. L. Henriksen, *J.Power Sources.* **2003**, *119–121*, 343–348.
[12] H. Köse, Ş. Karaal, A. O. Aydin, H. Akbulut, *Mat. Sci. Semicon. Proc.* **2015**, *38*, 404–412.
[13] M. Mohamedi, D. Takahashi, T. Itoh, I. Uchida, *Electrochim. Acta.* **2002**, *47*, 3483–3489.
[14] S. Zhang, K. Xu, T. Jow, *J. Solid State Electr.* **2003**, *7*, 147–151.
[15] S. S. Zhang, K. Xu, T. R. Jow, *J. Electrochem. Soc.* **2002**, *149,* A586-A590.
[16] S. S. Zhang, K. Xu, T. R. Jow, *J. Power Sources.* **2006**, *156*, 29–633.
[17] S. S. Zhang, K. Xu, T. R. Jow, *J. Power Sources.* **2006**, *159*, 702–707.
[18] L. D. Ellis, I. G. Hill, K. L. Gering, J. R. Dahn, *J. Electrochem. Soc.* **2017**, *164,* A2426-A2433.
[19] E. Zygadło-Monikowska, Z. Florjańczyk, P. Kubisa, T. Biedroń, A. Tomaszewska, J. Ostrowska, N. Langwald, *J. Power Sources.* **2010**, *195*, 6202–6206.
[20] H. Zhou, K. Xiao, J. Li, *J. Power Sources.* **2016**, *302,* 274–282.
[21] I. Shapiro, H. G. Weiss, *J. Am. Chem. Soc.* **1953**, *75,* 1753–1754.
[22] Z. Liu, J. Chai, G. Xu, Q. Wang, G. Cui, *Coordin. Chem. Rev.* **2015**, *292,* 56–73.
[23] H. G. Schweiger, M. Multerer, U. Wietelmann, J. C. Panitz, T. Burgemeister, H. J. Gores, *J. Electrochem. Soc.* **2005**, *152*, A622-A627.
[24] D. Aurbach, I. Weissman, A. Zaban, P. Dan, *Electrochim. Acta.* **1999**, *45*, 1135–1140.
[25] S. S. Zhang, K. Xu, T. R. Jow, *J. Power Sources.* **2006**, *156,* 629–633.
[26] M. Shanthi, C. M. Mathew, M. Ulaganathan, S. Rajendran, *Spectrochim. Acta A.* **2013**, *109,* 105–109.
[27] M. E. Jacox, W. E. Thompson, *J. Chem. Phys.* **2011**, *134,* 194306.
[28] X. Zheng, W. Wang, T. Huang, G. Fang, Y. Pan, M. Wu, *J. Power Sources.* **2016**, *329,* 450–455.
[29] X. Sun, J. Li, C. Shi, Z. Wang, E. Liu, C. He, X. Du, N. Zhao, *J. Power Sources.* **2012**, *220*, 264–268.
[30] R. Wang, X. Li, Z. Wang, H. Zhang, *Nano Energy.* **2017**, *34,* 131–140.
[31] Y. Qian, P. Niehoff, M. Börner, M. Grützke, X. Mönnighoff, P. Behrends, S. Nowak, M. Winter, F. M. Schappacher, *J. Power Sources.* **2016**, *329*, 31–40.
[32] M. Nie, B. L. Lucht, *J. Electrochem. Soc.* **2014**, *161*, A1001-A1006.
[33] P. Niehoff, M. Winter, *Langmuir.* **2013**, *29*, 15813–15821.
[34] K. Kim, I. Park, S.-Y. Ha, Y. Kim, M.-H. Woo, M.-H. Jeong, W. C. Shin, M. Ue, S. Y. Hong, N.-S. Choi, *Electrochim. Acta.* **2017**, *225,* 358–368.
[35] R. Wang, X. Li, Z. Wang, H. Guo, T. Hou, G. Yan, B. Huang, *J. Alloy Compd.* **2015**, *618,* 349–356.
[36] B. Wu, Y. Ren, D. Mu, X. Liu, G. Yang, F. Wu, *RCS Adv.* **2014**, *4*, 10196–10203.
[37] G. Yan, X. Li, Z. Wang, H. Guo, W. Peng, Q. Hu, J. Wang, *J. Solid State Electr.* **2017**, *21*, 1589-1597.

Submitted: January 5, 2019
Accepted: April 10, 2019